Archives of Hydro-Engineering and Environmental Mechanics
Vol. 50 (2003), No. 4, pp. 317–328

The Shape of Wetting Front in Soil Profile after Long-Drawn Imbibition

Krzysztof W. Książyński

Institute of Water Engineering and Water Management, Cracow University of Technology, ul. Warszawska 24, 31-155 Kraków, Poland e-mail: wksiazyn@smok.wis.pk.edu.pl

(Received May 16, 2002; revised June 30, 2003)

Abstract

In the paper a quasi-analytical formula for moisture increase along the wetting front during infiltration into a soil column is presented. Based on the formula, the moisture distribution along the column of six soils available in the literature was calculated. Then their verification was carried out using empirical data and the results obtained from other type models. The impact on the front shape of such factors as recharge rate, initial moisture content and direction of seepage against the vertical was checked.

Key words: wetting front, vadose zone, redistribution of moisture

1. Introduction

The increase of moisture content along the wetting front after long term imbibition is abrupt: moisture increases rapidly, mainly in the initial phase of wetting, when the soil is still comparatively dry (Olajossy, Siemek, Stopa 1990). What is more important in this phase of imbibition, is that the wetting profile undergoes practically no change during its movement in the column (Braester 1973). It can be assumed that in a certain system of coordinates connected with the front face, the shape of the moisture profile on the wetting front is approximately constant. The front face here is taken as a point where the increase of moisture is the highest.

Notation

c – differential water capacity [m^{-1}],
h_k – capillary head [m],
h – height of soil column [m],
h_s – suction head [m],
H – hydraulic head [m],

k – capillary conductivity [m/s],
k_0 – hydraulic conductivity (for full saturation) [m/s],
m – power index [–],
n – porosity coefficient [m^3/m^3],
p – water pressure in soil pores [N/m^2],
S – hydraulic slope [–],
t – time [s],
v – seepage velocity [m/s],
v_f – velocity of wetting front passage [m/s],
V – volume of water in the soil [m^3/m^2],
w – recharge rate of soil column [m/s],
w_0 – initial flow rate in soil column [m/s],
x, y, z – orthogonal coordinates [m],
Δx – finite increase of column length [m],
x_i – x coordinate of nod i of discrete net [m],
γ – specific weight of water [N/m^3],
φ – angle between flow direction and vertical [rad],
θ – soil moisture content [m^3/m^3],
$\Delta\theta$ – finite increase of moisture content [m^3/m^3],
θ_i – soil moisture content in nod i of discrete net [m^3/m^3],
$\theta_{\max}$ – maximum moisture content behind wetting front [m^3/m^3],
θ_n – soil moisture content at full saturation [m^3/m^3],
θ_0 – initial moisture content before wetting front [m^3/m^3],
θ_z – residual moisture content corresponding to the minimum conductivity of soil [m^3/m^3].

2. Velocity of the Wetting Front

The velocity of front movement can be calculated from water balance. For assumption that the axis x is consistent with the direction of seepage in the column, the volume of water in the soil down to a certain depth h can be described as

$$V = \int_h^0 \theta dx. \tag{1}$$

This quantity constantly increases with a speed $w - w_0$ arising from a recharge balance, and at the same time the front shifts down with velocity $v_f = dx/dt$. So the increase of water volume is equal to

$$\frac{dV}{dt} = \frac{d}{dt}\int_h^0 \theta dx = \int_h^0 \frac{d\theta}{dt} dx = \int_{\theta_0}^{\theta_{\max}} \frac{dx}{dt} d\theta = \\ = (\theta_{\max} - \theta_0)\, v_f = w - w_0. \tag{2}$$

From this equation one can get a formula for the front velocity:

$$v_f = \frac{w - w_0}{\theta_{\max} - \theta_0}. \tag{3}$$

It follows from relationship (3) that the lower is the change of the moisture content after front passage the higher is the velocity v_f. The value of $\theta_{\max}$ depends on the recharge rate and corresponds to the moisture content for the capillary conductivity equal to the recharge (Bouwer 1976, Bouwer 1978, Braester 1973):

$$k(\theta_{\max}) = w. \tag{4}$$

The recharge rate higher than the value of hydraulic conductivity results in the full saturation of the soil behind the wetting front, $\theta_{\max} = \theta_n$.

3. Analytical Description of Wetting Front

For one-dimensional movement the continuity equation can be written in the form:

$$-\frac{\partial v}{\partial x} = \frac{\partial \theta}{\partial t}. \tag{5}$$

Assuming the constant shape of wetting front one can conduct the following analysis: the moisture gradient at a chosen point is equal to $d\theta/dx$; after time dt the front will move down by a distance of $v_f\, dt$, while the moisture at the initial point will increase by the value $d\theta$ also described by the invariable front shape (Fig. 1). This results in the following relation between derivatives:

$$\frac{\partial \theta}{\partial t} = -v_f \frac{\partial \theta}{\partial x}. \tag{6}$$

Inserting relationship (6) into equation (5) one can obtain the formula:

$$v_f \frac{\partial \theta}{\partial x} = \frac{\partial v}{\partial x}. \tag{7}$$

Integration of both sides of this relation along the column length from its surface to arbitrary section x and for superficial seepage velocity $v(x = 0) = w$, gives:

$$\int_x^0 \frac{\partial v}{\partial x} dx = v_f \int_x^0 \frac{\partial \theta}{\partial x} dx \Rightarrow \int_v^w dv = v_f \int_\theta^{\theta_{\max}} d\theta \Rightarrow \\ \Rightarrow w - v = v_f\, (\theta_{\max} - \theta)\,. \tag{8}$$

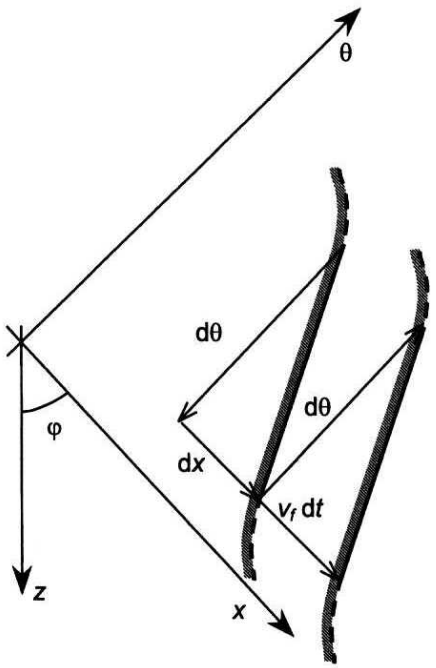

Fig. 1. Scheme of movement for invariable shape front

Inserting equation (3) one can determine the seepage velocity at an arbitrary point as a function of local moisture content:

$$v = w\left(1 - \frac{\theta_{\max} - \theta}{\theta_{\max} - \theta_0}\right) + w_0 \frac{\theta_{\max} - \theta}{\theta_{\max} - \theta_0}. \tag{9}$$

Darcy's formula affords the calculation of hydraulic slope:

$$S = -\frac{dH}{dx} = \frac{v}{k(\theta)} = \frac{w}{k(\theta)} \frac{\theta - \theta_0}{\theta_{\max} - \theta_0} + \frac{w_0}{k(\theta)} \frac{\theta_{\max} - \theta}{\theta_{\max} - \theta_0}. \tag{10}$$

The hydraulic head can be written in relation to the column direction as:

$$H = -z + \frac{p}{\gamma} = -x \cos\varphi - h_s. \tag{11}$$

After inserting this relationship into the formula for hydraulic slope the moisture decrease can be calculated as follows

$$\begin{aligned} \frac{d\theta}{dx} &= \frac{d\theta}{dh_s} \frac{dh_s}{dx} = -c(\theta)\left(-\cos\varphi - \frac{dH}{dx}\right) = \\ &= -c(\theta)\left[\frac{w}{k(\theta)} \frac{\theta - \theta_0}{\theta_{\max} - \theta_0} + \frac{w_0}{k(\theta)} \frac{\theta_{\max} - \theta}{\theta_{\max} - \theta_0} - \cos\varphi\right]. \end{aligned} \tag{12}$$

After inserting relationships $c(\theta)$ and $k(\theta)$ the formula (12) can be integrated along the column length and in this way the moisture profile for front can be determined. Because the integrated function is composite, adopting the numerical finite differences method for increases Δx and $\Delta\theta$ is more convenient (Książyński 1990):

$$x_i = x_{i+1} + \frac{\theta_{i+1} - \theta_i}{2}\left[\left(\frac{dx}{d\theta}\right)_i + \left(\frac{dx}{d\theta}\right)_{i+1}\right]. \tag{13}$$

4. Data used for Model Verification

To verify the method, data for six soils available in the literature were used, for which the shape of front moisture profile was determined. The shape was determined differently for different soils: for Castor sandy clay, Grenville silt clay, Northgouver clay and ABO/100 sand – from experiments, for Yolo light clay using quasi-analytical method and for Rehovot sand from calculations using a discrete diffusive model. Parameters of the moisture characteristic for these soils have been presented elsewhere (Książyński 2003), parameters of conductivity characteristics can be found in Table 1. Capillary conductivity was described by the Irmay-Averjanov formula (Averjanov 1950, Irmay 1954):

$$\frac{k}{k_0} = \left(\frac{\theta - \theta_z}{n - \theta_z}\right)^m. \tag{14}$$

Table 1. Soil parameters

Name of soil	n [%]	θ_z [%]	m	k_o [cm/d]	Source of measurement data
ABO/100	40	0	3.2	199	Zaradny 1977
Rehovot sand	38.7	0.45	4	1150	Rubin 1963
Yolo light clay	49.5	1.8	8.9	106	Philip 1957
Castor sandy clay	42.5	0.8	6.3	22	Staple 1966
Grenville silt clay	48	0	14.9	49	Staple 1966
Northgouver clay	52	4.4	19.8	177	Staple 1966

The front profile for ABO/100 sand (Zaradny 1977) was determined experimentally during capillary rise, infiltration and horizontal flow. For three clayey soils in natural state: Castor sandy clay, Grenville silt clay and Northgouver clay (Staple 1966) simple experimental profiles for infiltration were obtained. For Yolo light clay infiltration into vertical soil column was calculated using the quasi-analytical method of Philip (Philip 1957). The impact of different initial moisture content and different depths overtopping the soil surface were tested. For Rehovot sand, calculations of infiltration inside the vertical soil column were conducted using

the finite differences method, which resulted in the moisture profile description for different superficial recharge rate.

5. Verification of Formula for Front Moisture Profile

The correctness of formula (12) describing analytically the shape of the front profile was verified for four different soil types ranging from sand to clay for which laboratory measurements of moisture distribution during infiltration into a vertical soil column were made. Moreover, in order to be able to assess the impact of soil type on the front profile, only infiltration under full (or nearly full) saturation conditions was considered. Unfortunately, the recharge values in the available data were different and even relative values w/k_0 changed from 1.00 to 2.16. Initial moisture contents were also different although they were all close to the value of irreducible moisture. The results of experiments and calculations using formula (12) are presented in Fig. 2. The points denote measurement data, the lines representing the results of analytical calculations.

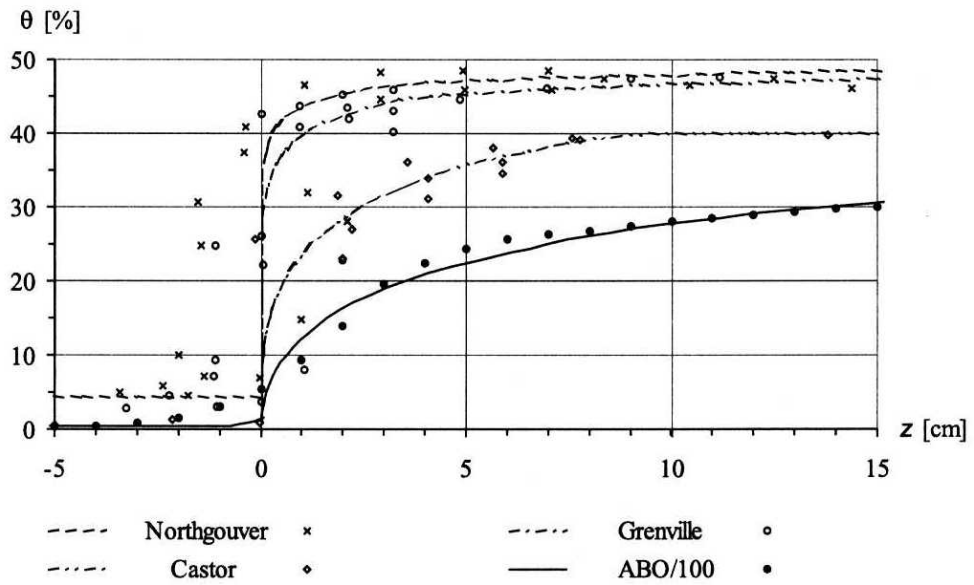

Fig. 2. Front shape for different soils

Infiltration in the Northgouver clay was carried out for surface recharge rate $w = 49$ cm/d. In consequence, a moisture content $\theta_{max} \cong 49\%$ appeared behind the front when the full saturation was $\theta_n = 52\%$. The initial moisture content was $\theta_0 = 4.4\%$. The results of measurements after 210 minutes of infiltration are presented in Fig. 2. As can be seen, the model fits the results of the experiment exactly, though the scatter of points on the front face is considerable. For all of

three natural soils such a wide range of measured moisture contents is typical and is connected with material heterogeneity caused by biological factors.

Infiltration into Grenville silt clay was run for an initial moisture $\theta_0 = 3\%$ without surface overtopping. The moisture content behind the front was close to the full saturation $\theta_n = 48\%$. Measurement results obtained after 135-minutes infiltration are presented. As before, the consistence between the model and experiment is good.

Infiltration into Castor sandy clay was run for initial moisture $\theta_0 = 0.8\%$ also without overtopping. The moisture content behind the front was close to full saturation $\theta_n = 42.5\%$. The results of calculations using formula (12) show conformity with the experiment similar to the previous one.

Infiltration into ABO/100 sand was run for initial moisture $\theta_0 = 0.5\%$ without superficial overtopping. The measurements were made 380 minutes after commencement of infiltration. The surface moisture content stopped at the level of 36.2% for full saturation $\theta_n = 40\%$. The experimental results conform well with analytical calculations. Thanks to the good homogeneity of the soil and the resulting accuracy of measurements, exact analysis of visible differences was possible. Despite similar values, the moisture gradient for an analytically designed front decreases with the distance from the face, while in reality it is almost constant along a certain length. The smooth increase of moisture before the front, not so clearly visible in the model, is also apparent.

In general, it can be stated that the analytical model reflects the true run of the wetting front quite well, which will also be confirmed further in the text on the basis of accordance with other verified models. At the same time the analytical formula makes a simple analysis of the reasons of formation of a given moisture profile possible, thus enabling us to foresee the variability of shape.

6. Impact of Initial Moisture on the Front Shape

The impact of initial moisture content on the front shape was tested for Yolo light clay for five different contents $\theta_0 = 0$, 6.2, 12.41, 23.76 and 36.63%. The moisture on the surface of the column was kept constant and close to the full saturation value $\theta_{max} = 48.21\%$. The shape of the front was determined after it attained steady form. The results obtained using quasi-analytical model and analytical calculations applying formula (12) are presented in Fig. 3. For convenience the quasi-analytical data are denoted by points, although in fact they are continuous and joined together by thin dashed lines. Numbers shown in the legend mean the value of initial moisture content.

The discrepancy of results is rather small, however, the front shape is apparently more regular in the analytical model. The greatest discrepancy was obtained for the highest initial moisture. In both models the front slope decreases identically together with the rise of the initial moisture. Also, in both cases, the highest

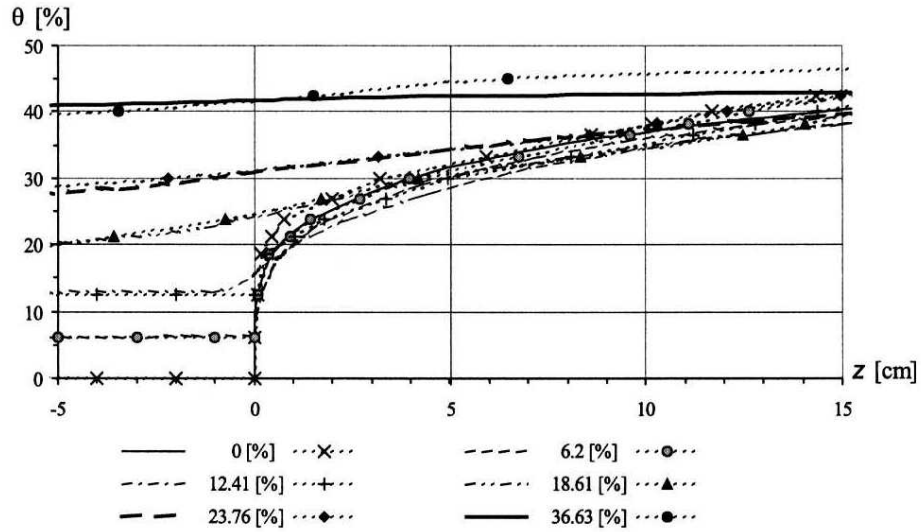

Fig. 3. Impact of initial moisture on front shape

moisture increase (the front face) appears for an increasingly higher moisture value – an increasingly visible broadening arises before the front face.

6.1. Impact of Recharge Rate on Front Shape

The analysis of the impact of the recharge on the front shape was made based on the results obtained during discrete model simulation of infiltration into Rehovot sand (Rubin 1963). Four different recharge rates were taken into account. Two of them: 251.4 [cm/h] (5.25 k_0) and 71.82 [cm/h] (1.5 k_0) ensured full saturation of soil, while the remaining – 4.7 [cm/h] (0.098 k_0) and 1.27 [cm/h] (0.027 k_0) – resulted in infiltration under unsaturated conditions. The initial moisture was θ_0 = 0.5%. For the verification only those results were applied which were obtained for the longest infiltration duration or for the moment of surface overtopping.

The results of discrete model simulation and analytical calculations using formula (12) are presented in Fig. 4. The legend is as for the previous figure, numbers stand for normalized infiltration rate w/k_0. The discrepancy of results for different values of recharge is also different although not greatly. The best consistency for the front shape and maximum moisture was obtained for the highest recharge. For the rate of order of 1.5 k_0 the discrepancy is the highest: the increase of moisture is evidently slower in the analytical model. On the other hand, the increase of moisture content for unsaturated infiltration, appearing near the front face, is faster for the analytical model, although the differences decrease at greater distances. Some of the discrepancies shown and the difference in the value of maximum saturation are the result of the low accuracy of reproducing

the conductivity characteristic by the Irmay-Averjanov formula for Rehovot sand. However, the correction of results with original characteristics is so small that the author abandoned its presentation. As expected, the front slope in both models increases together with recharge rate, which is also the reason for the moisture gradient decreasing during development of infiltration.

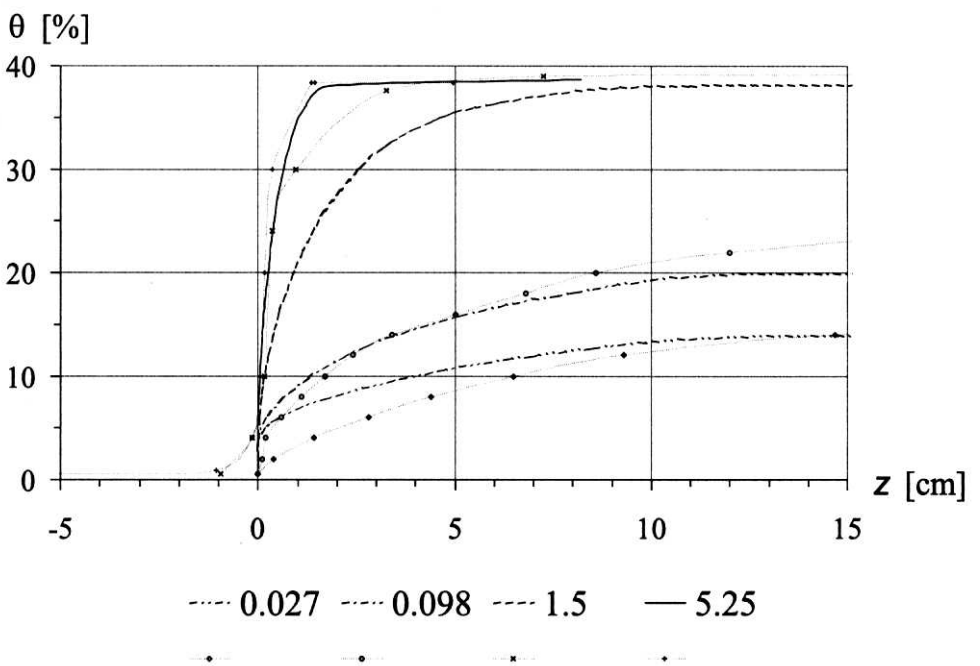

Fig. 4. Impact of a recharge rate on front shape

A similar analysis was also carried out for Yolo clay (Philip 1957) where the front shape used for purposes of comparison was determined from quasi-analytical computations for three different depths of water layer overtopping the surface. This corresponded to different recharge rates under other conditions of infiltration identical to those used in previous calculations for this soil. The influence of recharge was tested for three infiltration durations and for constant initial moisture content. As previously for Yolo clay, here also the discrepancy of results was not too high and the form of the front in analytical model was more regular. However, since the results were evidently better and brought nothing new into the matter, their presentation was abandoned.

7. Impact of Seepage Direction on Front Shape

Laboratory measurements of imbibition of ABO/100 sand (Zaradny 1977) made possible determination of the impact of seepage direction related to the vertical on the shape of the wetting front. The experiments were conducted for infiltration in a vertical column, for seepage into a horizontal column and for a capillary rise in a vertical column. To make more evident the differences between the seepage directions, early phases of the process were used for which hydraulic gradients were considerable, approximately the same and equal to ca. 220%. Both infiltration and capillary rise ran without overtopping the surface on which recharge covering the soil sorptivity takes place. Seepage in the horizontal column happens for the suction head on a recharge surface equal to 5 cm. The initial moisture was $\theta_0 = 0.5\%$. The results of measurements correspond to the process state after 350 minutes of infiltration, 250 minutes of horizontal seepage and 150 minutes of capillary rise. In Fig. 5 the results of experiments and analytical calculations using formula (12) where the value of angle φ was suitably changed, are presented. Measurement data are denoted by points and analytical results by lines in accordance with the symbols shown in the legend.

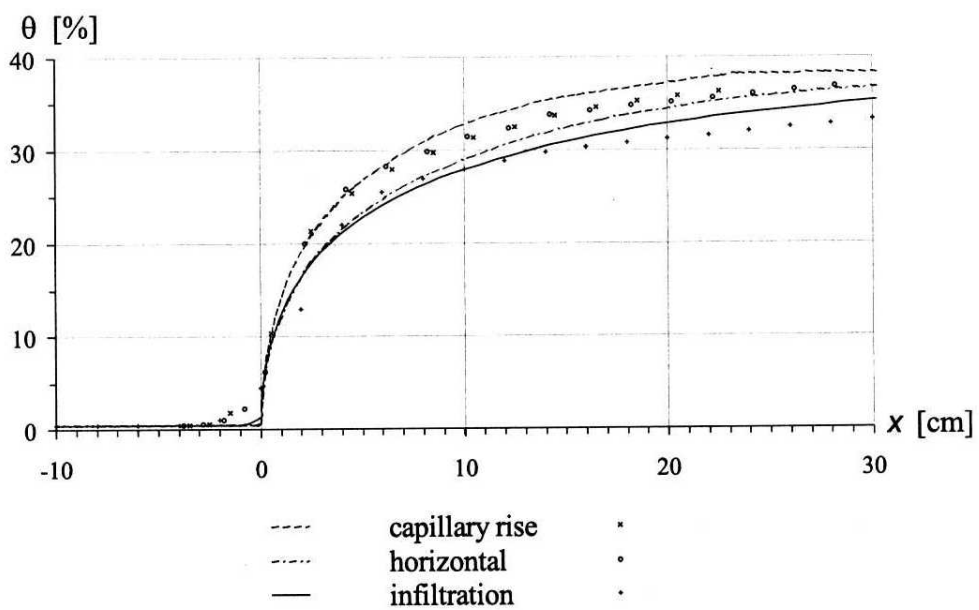

Fig. 5. Impact of seepage direction on front shape

As can be seen in Fig. 5, the front shape for a rise and horizontal flow are in reality very similar. The difference related to the front of infiltration in the

vertical column is also not too big. Under such conditions the analytical model, in spite of good results, does not reproduce moisture values precisely enough for them to be closer to the corresponding real curve than to another. Nevertheless, relations and other features typical for particular processes are mapped correctly. Despite the similar slope of the front, the differences in the shape are also visible: the slope of modelled front decreases with distance from the face, while in reality the slope is nearly constant along a certain length. A smooth increase of moisture before the front is also apparent, although not so clearly visible on the model.

8. Conclusions

Based on the presented results it can be found that the proposed analytical model reflects the real shape of the wetting front under different conditions quite well. Of course, using it to determine the moisture content course in the soil is purposeless, especially in the presence of efficient discrete models. However, the analytical description of the front makes possible easy recognition of reasons of its variability under different conditions and so to forecast the front shape for a wide range of parameters. In particular, it is possible to state under which conditions the use of the piston model is correct.

One can talk about the piston nature of the wetting front when very fast increase of moisture content (with an order of reciprocal of derivative of about 1 cm or higher) occurs on the front face. Such a situation took place for all investigated soils if low initial moisture contents occurred. The front zone, where moisture increases to the level of, say, 95% of θ_{max}, is quite narrow in sandy soils and also in natural clayey soils, especially for high recharge. In the case of Yolo clay, where the impact of high initial moisture values (above 10%) was tested, evident front broadening had already taken place. It results from the analytical model that this was caused by high values of conductivity and differential water capacity at the level of the initial condition. On the other hand, for low initial moisture the sharp front was formed even in the case of small recharge rate although average moisture gradients were then much lower. As results from the above observations, it is hard to talk about piston movement in case of recharge increasing if its earlier value had already been quite high.

The front broadening before its face is another question. A different range of that phenomenon is observed in various cases and its incorrect simulation with the models happens relatively often. The reason for the errors seems to be poor accuracy of calculations, which are based on empirical formulae of the capillary conductivity and moisture content for low moisture values. In consequence, for low initial moisture capillary conductivity often falls to zero, which means no water movement while in reality a small flow still takes place. As follows from formula (12), it is this flow that creates the front broadening before its face, as thanks to this the hydraulic gradient and hence the gradient of moisture are relatively low.

A similar event happened only for the ABO/100 sand where the front broadening for low moisture was evident (Fig. 2), although its range is smaller than in reality, which results from conductivity underestimated by the Irmay-Averjanov formula. For higher initial moisture contents empirical formulae follow soil characteristics more precisely and the broadening can be modelled better (Fig. 3).

References

Averjanov S. F. (1950), *About Permeability of Subsurface Soils in Case of Incomplete Saturation*, Eng. Collect 7.

Bouwer H. (1978), *Groundwater Hydrology*, McGraw-Hill, N. York.

Bouwer H. (1976), Infiltration into Increasingly Permeable Soils, *J. Irrig. Drain. Div., Am. Soc. Civ. Eng.*, 102, IR1, 127–136.

Braester C. (1973), Moisture Variation at the Soil Surface and the Advance of the Wetting Front during Infiltration at Constant Flux, *Water Resour. Res.* 3, 687–694.

Irmay S. (1954), On the Hydraulic Conductivity of Unsaturated Soils, *Eos Transactions of AGU* 35, 437–445.

Książyński K. (1990), Simplified Description of Water Infiltration through Vadose Zone (in Polish), *Gospodarka Wodna*, 50(4), 85–88.

Książyński K. (2003), Differential Water Capacity of Soil, *Archives of Hydro-engineering and Environmental Mechanics*, 50, No. 2, 75–84.

Olajossy A., Siemek J., Stopa J. (1990), Investigating Two-Phase Flows with Water in Porous Media using Microwave Techniques (in Polish), *Mechanika Płynów*: IX Konferencja Krajowa, ZG PK, Kraków, 251- 260.

Philip J. R. (1957), Numerical Solution of Equations of the Diffusion Type with Diffusivity Concentration-depend: 2, *Australian J. Phys.* 10, 29–42.

Rubin J., Steinhardt R. (1963), Soil Water Relations during Rain Infiltration, *J. Theory Soil Sci. Soc. Am. Proc.* 3.

Staple W. J., Gupta R. P. (1966), Infiltration into Homogeneous and Layered Columns of Aggregated Loam, Silt Loam and Slay Loam, *Canad. J. Soil Sci.* 46, 3.

Zaradny H. (1977), Modeling of Water Flow in the Vadose Zone (in Polish), *Rozprawy Hydrot.* 37, 83–131.